Cellular S-value of beta emitter radionuclide's determined using Geant4 Monte Carlo toolbox, comparison to MIRD S-values

Original Article

Mohammad Ali Tajik-Mansoury[1], Hossein Rajabi[1], Hossein Mozdarani[2]

[1]Department of Medical Physics, Faculty of Medical Sciences, Tarbiat Modares University, Tehran, Iran
[2]Department of Medical Genetics, Faculty of Medical Sciences, Tarbiat Modares University, Tehran, Iran

(Received 19 January 2015, Revised 2 October 2015, Accepted 14 October 2015)

ABSTRACT

Introduction: Spatial dose distribution around the radionuclides sources is required for optimized treatment planning in radioimmunotherapy. At present, the main source of data for cellular dosimetry is the s-values provided by MIRD. However, the MIRD s-values have been calculated based on analytical formula in which no electrons straggling is taken to account. In this study, we used Geant4-DNA Monte Carlo toolbox to calculate s-values and the results were compared to the corresponding MIRD data.

Methods: Similar to MIRD cell model, two concentric spheres representing the cell and its nucleus were used as the geometry of simulation. The cells were assumed to be made of water. Cellular s-values were calculated for three beta emitter radionuclides ^{131}I, ^{90}Y and ^{177}Lu that are widely used in radioimmunotherapy. Few lines of code in C++ were added into Geant4-DNA codes to automatically calculate the s-values and transfer data into excel files.

Results: The differences between two series of data were analyzed using Pearson's correlation and Bland-Altman curves. We observed high correlation (R^2>0.99) between two series of data for self-absorption; however, the agreement was very weak and Wilcoxon signed rank test showed significant difference (p-value<0.001). In cross-absorption, Bland-Altman analysis showed a considerable bias between MIRD s-values and corresponding Geant4-DNA data. The percent differences between the data were -79% to +67%.

Conclusion: Results of the comparison show a reflection of systematic error rather than statistical fluctuation. The inconsistency is most probably associated with the neglecting of straggling and δ-ray transport in MIRD analytical method.

Key words: Cellular S-value; Geant4-DNA; MIRD; Beta emitter; Radionuclides

Iran J Nucl Med 2016;24(1):37-45
Published: January, 2016
http://irjnm.tums.ac.ir

Corresponding author: Dr. Hossein Rajabi, Department of Medical physics, Faculty of Medical Sciences, Tarbiat Modares University, Tehran, Iran. E-mail: hrajabi@modares.ac.ir

INTRODUCTION

Ionizing radiation has an essential role in treatment of malignant diseases. External beam radiotherapy has been very effective in treatment of solid tumors however, inapplicable in management of disseminated small tumors and micro metastasis. Radionuclide therapy is a promising technique in treatment of such diseases. In radionuclide therapy, unsealed radionuclides are administrated to the patients for the selective delivery of radiation to the target cells [1]. The main issues in success of radionuclide therapy are proper choice of pharmaceutical for efficient targeting of the cancer cells and limiting the radiation dose to the targeted tumors. Monoclonal antibodies are the most specific targeting agents available and radioimmunotherapy as an advanced form of radionuclide therapy makes the use of these biomolecules to precisely hit the tumor cells [2-3]. However, confining the radiation dose to the cancer cells is a complicated task when the tumor size is very small. In such condition, the range of particles emitting from the radionuclide should be small to avoid damaged to surrounding normal tissues and at the same time, the absorbed dose to the tumors should be as uniform as possible for efficient treatment. Establishing such balance between particle range and size of tumor requires a good knowledge of spatial distribution of radiation dose around the radionuclide at microscopic levels [4-7]. Experimental dosimetry at this level is almost impossible and using some mathematical techniques is merely the only possibility [5, 8]. Two main techniques of internal dose estimation are analytical calculation and Monte Carlo simulation [9, 10].

Medical Internal Radiation Dose (MIRD) committee of the American society of nuclear medicine is at present the main source of analytically derived data at subcellular level. In 1997, MIRD published a book titled 'MIRD Cellular S Values' in which the S-values for self and the cross absorbed dose were provided for different cell compartments [11]. S-value is a concept devised by MIRD in 1965and is now very well-accepted model for internal dosimetry [12]. In MIRD scheme, tissues are categorized into the source and target and the absorbed dose in target region due to radiations from source region is calculated. S-value is the mean absorbed dose to the target region per unit cumulated activity in the source region (Gy/Bq.s) This concept was initially devised for dose estimation at organ level and later on extended to subcellular level analytical method based on MIRD primer formula [13]. The analytical calculation was based on Cole formula for electron range and stopping power [14] and the radiation spectra provided by Eckerman et al [15]. The MIRD book includes S-values for 262 radionuclides, several monoenergetic electrons (1 keV to 3 MeV) and α-particle (3 MeV to 10 MeV). The geometry for calculations was very simple, a homogeneous sphere (1-9 μm radius) representing the nucleus concentric within a spherical cell (3-10 μm radius). The principal compartments considered were nucleus, cytoplasm and cell surface.

Currently, Mote Carlo simulation is the most reliablemethod for tracking the transport of particles in nonhomogeneous materials and therefore, suitable for estimation of energy transfer from particles to the materials at microscopic level. Varieties of Monte Carlo codes with various degrees of sophistication are available and many of them have been used for cellular dosimetry [10, 16-21]. However, most of available Monte Carlo codes are developed based on condensed history algorithms and very few codes works based on track structure technique. In condense history technique, the particle's track are divide into small segments and the interactions along the tracks are average at the end of each segment while, in track structure technique, all the interactions in an event-by-event manner are considered [22]. Theoretically, track structure Monte Carlo codes provide more accurate results compared to condense history codes nevertheless, no published data are available with this type of Monte Carlo codes.

At present, the only freely available track structure Monte Carlo code is Geant4-DNA that is a part of general purpose Geant4 code. The Geant4-DNA was originally initiated by the European Space Agency/ESTEC for the modeling of early biological damage induced by ionizing radiation at molecular scale (DNA scale). The development is now going on in the framework of the Geant4-DNA project [23].

In the present study, we determined S-values using Geant4-DNA track structure Monte Carlo code and the results were compared to corresponding data published by MIRD. Three commonly used β-emitter radionuclides ^{131}I, ^{90}Y and ^{177}Lu were considered for this comparison.

METHODS

Decay scheme of radionuclides

The radiation spectra form ^{131}I, ^{90}Y and ^{177}Lu were set exactly based on the information given in 'MIRD: Radionuclide Data and Decay Schemes [24]. Summary of the decay schemes for these radionuclides are shown in Table 1. The table includes the number, the average energy and the total yield of each particle. As per Geant4 procedure, for each radionuclide three radiation spectra were defined, one discrete spectrum for photons (gamma, x-ray), one continuous spectrum for β-emission and one discrete spectrum for δ-particles (Auger, internal conversion).

Geant4-DNA Mote Carlo code

We used Geant4 (Version 4.10.1) as the Monte Carlo simulator [25]. In this simulation, we used Geant4-DNA that covers electron interactions down to 7.4 eV. Below this energy level, particle tacking was terminated and the kinetic energy was absorbed at the spot. All the Geant4-DNA physics discrete process were taken into account including; ionization, electronic excitation, vibrational excitation, elastic scattering and molecular attachment for interactions. Simulations were performed on a PC (Intel® Core™ i7 Processors) with Linux (fedora 19) operating systemand no variance- reduction techniquewas used in the simulations.

Geometry of simulation for calculation of S-values

The cell geometry in this study was exactly similar to the MIRD model that is, two concentric spheres of different radiuses, Figure 1[11].

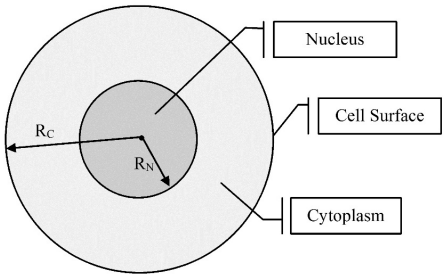

Fig 1. MIRD geometric model for cell compartments, R_C and R_N indicate cell and nucleus radius, respectively [11].

The radius of the cell and nucleus were 3-10 µm and 1-9 µm, respectively. This cell sizes were selected in order to compare the results with MIRD data. Similar to MIRD, we assumed the cells composed of unit density water (G4_WATER in Geant4-DNA jargon). Radionuclides were assumed uniformly distributed in one of the cell compartments; over the cell surface (Cs), inside the cytoplasm (Cy) and inside the cell nucleus (N).

Data acquisition and processing

27 realizations of the cell models were generated and radionuclides were independently considered in one of the 3 cell compartments. For each radionuclide 81 simulation (27×3) were performed. In all the simulations (81×3), hundred thousand radionuclides decays were considered to assure statistical uncertainty of below 5%. A few lines of codes (C++) were added into the Geant4 code to perform the necessary calculations and save the data in binary format in hard disk. The relative percentage difference between our results and corresponding MIRD data was calculated as:

$$RD\% = 100 \times \left(1 - \frac{S\text{-value}_{Geant4}}{S\text{-value}_{MIRD}}\right)$$

This definition can go over 100%.

RESULTS

The S-values derived for ^{131}I, ^{177}Lu and ^{90}Y in cell compartments are presented in Tables 1, 2 and 3, respectively. For the sake of easy comparison, the corresponding MIRD S-values and percent differences (RD %) are also included in the tables. The first and second columns of tables are the radius of cells (R_C) and radius of nucleus (R_N) respectively. Tables include S-values for the self-absorption from cell to cell (C←C) and nucleus to nucleus (N←N) that are presented in the left part of the tables. The S-values for the cross-absorption including cell-surface to cell (C←C_S), cytoplasm to nucleus (N←Cy) and cell-surface to nucleus (N←C_S) are presented on the right part of the tables.

Comparison of self-absorption S-values

The scatter plots of the self-absorption data and the linear curves fitted to the data is shown in Figure 2.

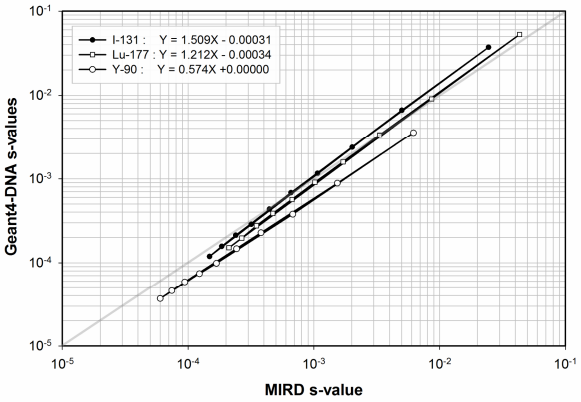

Fig 2. The scatter plot and Pearson's correlation analyses of the S-values derived with Geant4-DNA and MIRD published data for ^{131}I, ^{177}Lu and ^{90}Y. For better visual perception, graphs are shown in full logarithmic scale.

Due to long range of S-values and for better visual perception, graphs in Figure 2 are shown in full-logarithmic scale. A quick look at the figure reveals extremely low statistical variation and very high correlation between MIRD and Geant4-DNA data. Irrespective of high linear Pearson's correlation (R^2>0.99), Wilcoxon signedrank testshowed significant difference between the MIRD and Geant4-DNA S-values (p-values <0.001).

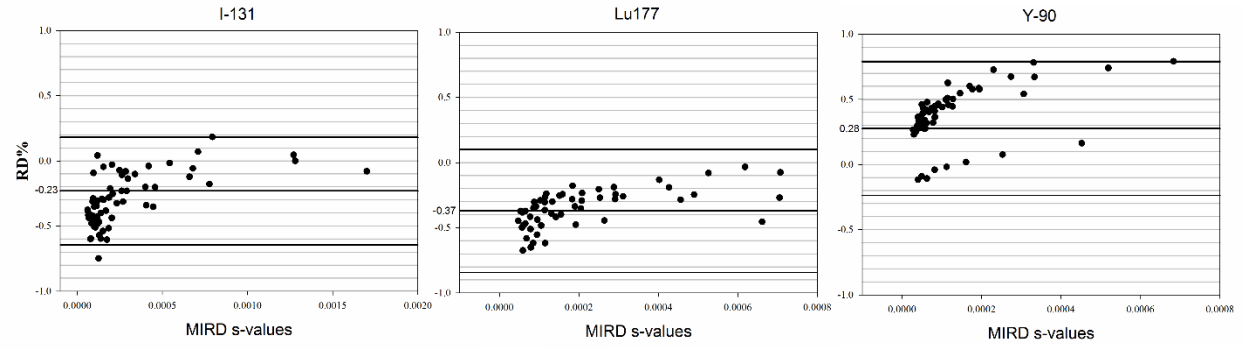

Fig 3. The Bland-Altman graphs for analyzing the agreement between cross-absorption S-values derived with Geant4-DNA and MIRD published data for ^{131}I, ^{177}Lu and ^{90}Y.

Table 1: Summary of decay schemes for radionuclides, including the number of particles and the mean energy released per disintegration.

	^{131}I			^{177}Lu			^{90}Y		
Radiation	No.	E_{mean} (keV)	Total yield	No.	E_{mean} (keV)	Total yield	No.	E_{mean} (keV)	Total yield
Gamma	19	3.812E+02	1.008E+00	6	3.16E+01	1.803E-01	1	3.06E-05	1.000E-08
x-ray	49	1.522E-03	8.175E-01	60	3.54E+00	1.374E+00	40	1.20E-03	1.466E-03
β-particles	6	1.819E+02	1.000E+00	40	1.33E+02	1.000E+00	3	9.33E+02	1.000E+00
IC electrons	108	9.567E+00	6.458E-02	36	1.35E+01	1.548E-01	10	2.01E-01	1.150E-04
Auger electrons	13	4.129E-01	6.975E-01	15	1.83E+02	1.117E+00	11	6.55E-04	1.273E-03

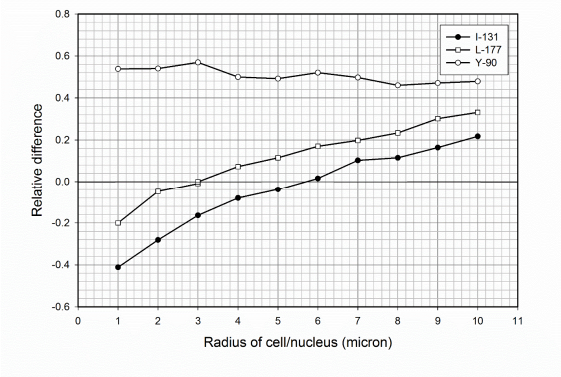

Fig 4. The relative percentage difference (RD%) in S-values derived with Geant4-DNA and MIRD published data for ^{131}I, ^{177}Lu and ^{90}Y.

The equations of fitted curves to the data are shown in the figure legend. As seen, the slopes of the curves are considerably different from unity, representing systematic differences between MIRD and Geant4-DNA S-values. The slopes of linear curves are 1.509, 1.212 and 0.574 for ^{131}I, ^{177}Lu and ^{90}Y respectively. Slopes are the average relative difference between Geant4-DNA and MIRD data. Slopes of ^{131}I and ^{177}Lu curves are greater than unity and the corresponding intercepts are negative. These curves intersect the unity line approximately at 0.0006 and 0.0016 respectively. It means that S-values calculated by Geant4-DNA are smaller than the MIRD values below these values and larger above these values.

The magnitude of S-values depended on the type of radiation and its relative yield. It also depends on the size and material composition of the source region. Based on the data in Tables 2, 3 and 4, as the size of cell/nucleus increases the magnitude of self-absorption S-values decreases. The relative differences between two series of data versus the size of source regions are shown in Figure 4.

Comparison of cross-absorption S-values

The bland-Altman of the cross-absorption S-values are presented in Figure 3. Although all the data points are in the limit of agreements (1.98×standard deviation), there are considerable bias between MIRD S-values and corresponding Geant4-DNA data. The biases for ^{131}I, ^{177}Lu and ^{90}Y were -23%, -37% and +28% respectively. The biases were in opposite direction compared to self-absorption that is, where the self-absorption estimated by Geant4-DNA were higher than MIRD corresponding S-values the cross-absorption were lower and vice versa.

Table 2: Cellular S-value for ^{131}I from MIRD and Geant4-DNA calculation.

Radius		Self-absorption						Cross-absorption								
R_C	R_N	S(C←C)			S(N←N)			S(C←Cs)			S(N←Cy)			S(N←Cs)		
(μm)	(μm)	MIRD	Geant4	RD%	MIRD	Geant4	RD%	MIRD	Geant4	RD%	MIRD	Geant4	RD%	MIRD	Geant4	RD%
3	1	2.02E-03	2.38E-03	-18%	2.45E-02	3.72E-02	-52%	1.27E-03	1.33E-03	-5%	1.70E-03	1.57E-03	8%	7.09E-04	7.61E-04	-7%
3	2	2.02E-03	2.38E-03	-18%	5.01E-03	6.65E-03	-33%	1.27E-03	1.33E-03	-5%	1.28E-03	1.28E-03	0%	7.76E-04	6.49E-04	16%
4	2	1.07E-03	1.16E-03	-8%	5.01E-03	6.65E-03	-33%	6.79E-04	6.41E-04	6%	7.93E-04	9.53E-04	-20%	4.05E-04	2.87E-04	29%
4	3	1.07E-03	1.16E-03	-8%	2.02E-03	2.38E-03	-18%	6.79E-04	6.41E-04	6%	6.59E-04	5.83E-04	12%	4.46E-04	3.12E-04	30%
5	2	6.57E-04	6.83E-04	-4%	5.01E-03	6.65E-03	-33%	4.19E-04	4.03E-04	4%	5.42E-04	5.33E-04	2%	2.48E-04	2.31E-04	7%
5	3	6.57E-04	6.83E-04	-4%	2.02E-03	2.38E-03	-18%	4.19E-04	4.03E-04	4%	4.57E-04	3.73E-04	18%	2.63E-04	2.36E-04	10%
5	4	6.57E-04	6.83E-04	-4%	1.07E-03	1.16E-03	-8%	4.19E-04	4.03E-04	4%	4.00E-04	3.27E-04	18%	2.90E-04	2.30E-04	21%
6	3	4.43E-04	4.36E-04	2%	2.02E-03	2.38E-03	-18%	2.84E-04	2.62E-04	8%	3.39E-04	3.06E-04	10%	1.74E-04	9.32E-05	46%
6	4	4.43E-04	4.36E-04	2%	1.07E-03	1.16E-03	-8%	2.84E-04	2.62E-04	8%	2.97E-04	2.59E-04	13%	1.85E-04	1.09E-04	41%
6	5	4.43E-04	4.36E-04	2%	6.57E-04	6.83E-04	-4%	2.84E-04	2.62E-04	8%	2.69E-04	1.96E-04	27%	2.03E-04	1.30E-04	36%
7	3	3.18E-04	2.87E-04	10%	2.02E-03	2.38E-03	-18%	2.04E-04	1.98E-04	3%	2.61E-04	2.07E-04	21%	1.25E-04	5.69E-05	54%
7	4	3.18E-04	2.87E-04	10%	1.07E-03	1.16E-03	-8%	2.04E-04	1.98E-04	3%	2.32E-04	1.67E-04	28%	1.30E-04	7.22E-05	44%
7	5	3.18E-04	2.87E-04	10%	6.57E-04	6.83E-04	-4%	2.04E-04	1.98E-04	3%	2.08E-04	1.61E-04	23%	1.38E-04	7.46E-05	46%
7	6	3.18E-04	2.87E-04	10%	4.43E-04	4.36E-04	2%	2.04E-04	1.98E-04	3%	1.93E-04	1.56E-04	19%	1.51E-04	8.69E-05	42%
8	4	2.39E-04	2.13E-04	11%	1.07E-03	1.16E-03	-8%	1.54E-04	1.47E-04	5%	1.86E-04	1.40E-04	25%	9.64E-05	6.03E-05	37%
8	5	2.39E-04	2.13E-04	11%	6.57E-04	6.83E-04	-4%	1.55E-04	1.47E-04	5%	1.68E-04	1.14E-04	32%	1.00E-04	5.97E-05	40%
8	6	2.39E-04	2.13E-04	11%	4.43E-04	4.36E-04	2%	1.54E-04	1.47E-04	5%	1.54E-04	1.14E-04	26%	1.06E-04	6.29E-05	41%
8	7	2.39E-04	2.13E-04	11%	3.18E-04	2.87E-04	10%	1.54E-04	1.47E-04	5%	1.45E-04	1.08E-04	26%	1.16E-04	7.05E-05	39%
9	5	1.85E-04	1.57E-04	15%	6.57E-04	6.83E-04	-4%	1.19E-04	1.24E-04	-4%	1.39E-04	9.26E-05	33%	7.69E-05	4.14E-05	46%
9	6	1.85E-04	1.57E-04	15%	4.43E-04	4.36E-04	2%	1.19E-04	1.24E-04	-4%	1.28E-04	7.93E-05	38%	8.00E-05	4.32E-05	46%
9	7	1.85E-04	1.57E-04	15%	3.18E-04	2.87E-04	10%	1.19E-04	1.24E-04	-4%	1.19E-04	8.74E-05	27%	8.47E-05	5.20E-05	39%
9	8	1.85E-04	1.57E-04	15%	2.39E-04	2.13E-04	11%	1.19E-04	1.24E-04	-4%	1.13E-04	7.96E-05	30%	9.23E-05	6.00E-05	35%
10	5	1.48E-04	1.19E-04	20%	6.57E-04	6.83E-04	-4%	9.55E-05	8.70E-05	9%	1.17E-04	7.56E-05	35%	6.09E-05	4.16E-05	32%
10	6	1.48E-04	1.19E-04	20%	4.43E-04	4.36E-04	2%	9.55E-05	8.70E-05	9%	1.08E-04	7.64E-05	29%	6.27E-05	4.24E-05	32%
10	7	1.48E-04	1.19E-04	20%	3.18E-04	2.87E-04	10%	9.55E-05	8.70E-05	9%	1.00E-04	7.00E-05	30%	6.52E-05	4.27E-05	35%
10	8	1.48E-04	1.19E-04	20%	2.39E-04	2.13E-04	11%	9.55E-05	8.70E-05	9%	9.41E-05	7.03E-05	25%	6.90E-05	4.41E-05	36%
10	9	1.48E-04	1.19E-04	20%	1.85E-04	1.57E-04	15%	9.55E-05	8.70E-05	9%	9.02E-05	6.59E-05	27%	7.50E-05	4.93E-05	34%

Table 3: Cellular S-value for ^{177}Lu from MIRD and Geant4-DNA calculation.

Radius		Self-absorption						Cross-absorption								
R_C	R_N	S(C←C)			S(N←N)			S(C←Cs)			S(N←Cy)			S(N←Cs)		
(μm)	(μm)	MIRD	Geant4	RD%	MIRD	Geant4	RD%	MIRD	Geant4	RD%	MIRD	Geant4	RD%	MIRD	Geant4	RD%
3	1	3.34E-03	3.37E-03	-1%	4.32E-02	5.28E-02	-22%	2.04E-03	2.21E-03	-8%	2.73E-03	3.14E-03	-15%	9.25E-04	7.05E-04	24%
3	2	3.34E-03	3.37E-03	-1%	8.64E-03	9.07E-03	-5%	2.04E-03	2.21E-03	-8%	2.02E-03	2.08E-03	-3%	1.11E-03	8.46E-04	24%
4	2	1.71E-03	1.59E-03	7%	8.64E-03	9.07E-03	-5%	1.05E-03	6.61E-04	37%	1.16E-03	1.30E-03	-12%	5.17E-04	4.27E-04	17%
4	3	1.71E-03	1.59E-03	7%	3.34E-03	3.37E-03	-1%	1.05E-03	6.61E-04	37%	9.74E-04	9.23E-04	5%	6.08E-04	4.56E-04	25%
5	2	1.02E-03	9.09E-04	11%	8.64E-03	9.07E-03	-5%	6.28E-04	4.90E-04	22%	7.62E-04	7.07E-04	7%	3.12E-04	1.92E-04	38%
5	3	1.02E-03	9.09E-04	11%	3.34E-03	3.34E-03	0%	6.28E-04	4.90E-04	22%	6.39E-04	6.18E-04	3%	3.32E-04	2.53E-04	24%
5	4	1.02E-03	9.09E-04	11%	1.71E-03	1.59E-03	7%	6.28E-04	4.90E-04	22%	5.70E-04	5.26E-04	8%	3.86E-04	2.91E-04	25%
6	3	6.71E-04	5.66E-04	16%	3.34E-03	3.34E-03	0%	4.15E-04	2.64E-04	36%	4.59E-04	4.02E-04	12%	2.18E-04	1.15E-04	47%
6	4	6.71E-04	5.66E-04	16%	1.71E-03	1.59E-03	7%	4.15E-04	2.64E-04	36%	4.04E-04	3.11E-04	23%	2.32E-04	1.55E-04	33%
6	5	6.71E-04	5.66E-04	16%	1.02E-03	9.09E-04	11%	4.15E-04	2.64E-04	36%	3.73E-04	2.92E-04	22%	2.67E-04	1.90E-04	29%
7	3	4.72E-04	3.87E-04	18%	3.34E-03	3.34E-03	0%	2.93E-04	2.05E-04	30%	3.48E-04	2.88E-04	17%	1.55E-04	7.88E-05	49%
7	4	4.72E-04	3.87E-04	18%	1.71E-03	1.59E-03	7%	2.93E-04	2.05E-04	30%	3.07E-04	2.50E-04	19%	1.61E-04	8.50E-05	47%
7	5	4.72E-04	3.87E-04	18%	1.02E-03	9.09E-04	11%	2.93E-04	2.05E-04	30%	2.78E-04	2.07E-04	26%	1.72E-04	1.05E-04	39%
7	6	4.72E-04	3.87E-04	18%	6.71E-04	5.66E-04	16%	2.93E-04	2.05E-04	30%	2.63E-04	2.08E-04	21%	1.95E-04	1.31E-04	33%
8	4	3.49E-04	2.76E-04	21%	1.71E-03	1.59E-03	7%	2.17E-04	1.42E-04	35%	2.43E-04	1.83E-04	25%	1.19E-04	5.90E-05	50%
8	5	3.49E-04	2.76E-04	21%	1.02E-03	9.09E-04	11%	2.17E-04	1.42E-04	35%	2.20E-04	1.84E-04	16%	1.24E-04	6.81E-05	45%
8	6	3.49E-04	2.76E-04	21%	6.71E-04	5.66E-04	16%	2.17E-04	1.42E-04	35%	2.03E-04	1.59E-04	22%	1.32E-04	7.83E-05	41%
8	7	3.49E-04	2.76E-04	21%	4.72E-04	3.87E-04	18%	2.17E-04	1.42E-04	35%	1.95E-04	1.51E-04	23%	1.49E-04	9.54E-05	36%
9	5	2.67E-04	1.97E-04	26%	1.02E-03	9.09E-04	11%	1.67E-04	9.45E-05	43%	1.80E-04	1.33E-04	26%	9.47E-05	5.69E-05	40%
9	6	2.67E-04	1.97E-04	26%	6.71E-04	5.66E-04	16%	1.67E-04	9.45E-05	43%	1.65E-04	1.14E-04	31%	9.88E-05	6.05E-05	39%
9	7	2.67E-04	1.97E-04	26%	4.72E-04	3.87E-04	18%	1.67E-04	9.45E-05	43%	1.55E-04	1.14E-04	26%	1.05E-04	6.52E-05	38%
9	8	2.67E-04	1.97E-04	26%	3.49E-04	2.76E-04	21%	1.67E-04	9.45E-05	43%	1.50E-04	1.15E-04	23%	1.18E-04	7.73E-05	34%
10	5	2.11E-04	1.51E-04	28%	1.02E-03	9.09E-04	11%	1.32E-04	4.31E-05	67%	1.50E-04	1.18E-04	21%	7.46E-05	4.73E-05	37%
10	6	2.11E-04	1.51E-04	28%	6.71E-04	5.66E-04	16%	1.32E-04	4.31E-05	67%	1.38E-04	1.03E-04	25%	7.70E-05	5.28E-05	31%
10	7	2.11E-04	1.51E-04	28%	4.72E-04	3.87E-04	18%	1.32E-04	4.31E-05	67%	1.29E-04	9.18E-05	29%	8.04E-05	5.51E-05	31%
10	8	2.11E-04	1.51E-04	28%	3.49E-04	2.76E-04	21%	1.32E-04	4.31E-05	67%	1.22E-04	8.57E-05	30%	8.54E-05	5.80E-05	32%
10	9	2.11E-04	1.51E-04	28%	2.67E-04	1.97E-04	26%	1.32E-04	4.31E-05	67%	1.19E-04	8.77E-05	26%	9.52E-05	6.53E-05	31%

Table 4: Cellular S-value for ^{90}Y from MIRD and Geant4-DNA calculation.

Radius		Self-absorption						Cross-absorption								
R_C	R_N	S(C←C)			S(N←N)			S(C←Cs)			S(N←Cy)			S(N←Cs)		
(μm)	(μm)	MIRD	Geant4	RD%	MIRD	Geant4	RD%	MIRD	Geant4	RD%	MIRD	Geant4	RD%	MIRD	Geant4	RD%
3	1	6.79E-04	3.78E-04	57%	6.20E-03	3.57E-03	54%	4.52E-04	5.33E-04	-16%	6.83E-04	1.58E-03	-79%	3.06E-04	5.33E-04	-54%
3	2	6.79E-04	3.78E-04	57%	1.54E-03	8.85E-04	54%	4.52E-04	5.33E-04	-16%	5.19E-04	1.13E-03	-74%	3.33E-04	6.70E-04	-67%
4	2	3.80E-04	2.28E-04	50%	1.54E-03	8.85E-04	54%	2.53E-04	2.73E-04	-8%	3.31E-04	7.57E-04	-78%	1.77E-04	3.21E-04	-58%
4	3	3.80E-04	2.28E-04	50%	6.79E-04	3.78E-04	57%	2.53E-04	2.73E-04	-8%	2.74E-04	5.53E-04	-67%	1.93E-04	3.53E-04	-59%
5	2	2.43E-04	1.47E-04	49%	1.54E-03	8.85E-04	54%	1.61E-04	1.64E-04	-2%	2.30E-04	4.93E-04	-73%	1.10E-04	1.83E-04	-50%
5	3	2.43E-04	1.47E-04	49%	6.79E-04	3.78E-04	57%	1.61E-04	1.64E-04	-2%	1.95E-04	3.53E-04	-58%	1.16E-04	1.85E-04	-46%
5	4	2.43E-04	1.47E-04	49%	3.80E-04	2.28E-04	50%	1.61E-04	1.64E-04	-2%	1.70E-04	3.16E-04	-60%	1.27E-04	2.00E-04	-45%
6	3	1.68E-04	9.86E-05	52%	6.79E-04	3.78E-04	57%	1.12E-04	1.10E-04	2%	1.46E-04	2.56E-04	-55%	7.80E-05	1.08E-04	-32%
6	4	1.68E-04	9.86E-05	52%	3.80E-04	2.28E-04	50%	1.12E-04	1.10E-04	2%	1.28E-04	2.14E-04	-50%	8.23E-05	1.19E-04	-36%
6	5	1.68E-04	9.86E-05	52%	2.43E-04	1.47E-04	49%	1.12E-04	1.10E-04	2%	1.15E-04	2.20E-04	-63%	8.98E-05	1.43E-04	-46%
7	3	1.23E-04	7.40E-05	50%	6.79E-04	3.78E-04	57%	8.19E-05	7.87E-05	4%	1.14E-04	1.92E-04	-51%	5.63E-05	7.43E-05	-28%
7	4	1.23E-04	7.40E-05	50%	3.80E-04	2.28E-04	50%	8.19E-05	7.87E-05	4%	1.01E-04	1.58E-04	-44%	5.83E-05	7.70E-05	-28%
7	5	1.23E-04	7.40E-05	50%	2.43E-04	1.47E-04	49%	8.19E-05	7.87E-05	4%	9.09E-05	1.46E-04	-47%	6.15E-05	8.49E-05	-32%
7	6	1.23E-04	7.40E-05	50%	1.68E-04	9.86E-05	52%	8.19E-05	7.87E-05	4%	8.35E-05	1.32E-04	-45%	6.69E-05	1.01E-04	-41%
8	4	9.41E-05	5.89E-05	46%	3.80E-04	2.28E-04	50%	6.25E-05	5.61E-05	11%	8.19E-05	1.24E-04	-41%	4.37E-05	5.79E-05	-28%
8	5	9.41E-05	5.89E-05	46%	2.43E-04	1.47E-04	49%	6.25E-05	5.61E-05	11%	7.41E-05	1.15E-04	-43%	4.53E-05	6.02E-05	-28%
8	6	9.41E-05	5.89E-05	46%	1.68E-04	9.86E-05	52%	6.25E-05	5.61E-05	11%	6.78E-05	1.02E-04	-40%	4.78E-05	6.43E-05	-29%
8	7	9.41E-05	5.89E-05	46%	1.23E-04	7.40E-05	50%	6.25E-05	5.61E-05	11%	6.32E-05	1.03E-04	-48%	5.19E-05	7.23E-05	-33%
9	5	7.42E-05	4.59E-05	47%	2.43E-04	1.47E-04	49%	4.93E-05	4.51E-05	9%	6.17E-05	9.44E-05	-42%	3.50E-05	4.52E-05	-25%
9	6	7.42E-05	4.59E-05	47%	1.68E-04	9.86E-05	52%	4.93E-05	4.51E-05	9%	5.66E-05	7.99E-05	-34%	3.63E-05	4.82E-05	-28%
9	7	7.42E-05	4.59E-05	47%	1.23E-04	7.40E-05	50%	4.93E-05	4.51E-05	9%	5.25E-05	8.17E-05	-44%	3.83E-05	5.16E-05	-30%
9	8	7.42E-05	4.59E-05	47%	9.41E-05	5.89E-05	46%	4.93E-05	4.51E-05	9%	4.96E-05	7.93E-05	-46%	4.14E-05	5.80E-05	-33%
10	5	6.00E-05	3.68E-05	48%	2.43E-04	1.47E-04	49%	3.99E-05	3.55E-05	12%	5.22E-05	7.77E-05	-39%	2.78E-05	3.64E-05	-27%
10	6	6.00E-05	3.68E-05	48%	1.68E-04	9.86E-05	52%	3.99E-05	3.55E-05	12%	4.82E-05	7.02E-05	-37%	2.86E-05	3.73E-05	-26%
10	7	6.00E-05	3.68E-05	48%	1.23E-04	7.40E-05	50%	3.99E-05	3.55E-05	12%	4.47E-05	5.94E-05	-28%	2.98E-05	3.76E-05	-23%
10	8	6.00E-05	3.68E-05	48%	9.41E-05	5.89E-05	46%	3.99E-05	3.55E-05	12%	4.19E-05	5.86E-05	-33%	3.13E-05	4.02E-05	-25%
10	9	6.00E-05	3.68E-05	48%	7.42E-05	4.59E-05	47%	3.99E-05	3.55E-05	12%	3.99E-05	5.77E-05	-36%	3.38E-05	4.41E-05	-26%

The band-Altman graphs for ^{90}Y shows two different trends in data values rather than statistical variation. The data points in lower part of graph are the S-values for cell-surface to nucleus ($C \leftarrow C_S$) with -0.04% bias.

DISCUSSION

Interaction of primary and secondary electrons with atoms is the main mechanism of energy transfer from radiation to matter. The track structure Monte Carlo techniques were developed for precise simulate of electron transport in water, the main material in living organisms [26]. Geant4-DNA is the only track structure code freely available. Geant4-DNA has been verified for the transport of electrons in water, calculation of the stopping power and the range of electrons and the published reports confirm good agreement with other dedicated track structure codes [27-30]. Track structure Monte Carlo codes can be used for microscopic dose estimation however, require a tremendous amount of time and were rarely used for this purposes and therefore there is no significant publication. In the present study, we derived cellular S-values using Geant4-DNA Mote Carlo code and compared the results to the MIRD published data [11]. The objective was to reveal the systematic errors in the MIRD S-values. We selected three widely used therapeutic radionuclides that have quite different radiation spectra. Regarding the photon emission, ^{131}I has the high energy gamma photons (E_{mean} =381 keV) of high yield, radionuclide ^{90}Y has almost no gamma emission and the energy of ^{177}Lu gamma photons are somewhere in between (E_{mean} =32 keV). On the contrary, ^{90}Y has very high energy β-emission (E_{mean}=933 keV) while ^{131}I and ^{177}Lu emit medium energy β-radiations (181 and 133 keV, respectively). The x-rays, internal conversion and Auger electrons from these radionuclides have very low energy and are effective only at very short ranges. We analyzed the results for self-absorption and cross absorption independently because, self-absorption is mainly due to short range electrons and cross-absorption is due to long range electrons and low energy photons.

For ^{90}Y data, the self-absorption S-values calculated by Geant4-DNA are almost half of the MIRD data. However, for cross-absorption MIRD data have higher values with positive bias of 28%. Bland-Altman graph shows a systematic rather than statistical difference between the cross-absorption for this radionuclide. The bias for ($C \leftarrow C_S$) was -0.04% and for both ($N \leftarrow C_y$) and ($N \leftarrow C_S$) was +43%. There is no explanation for this inconsistency except error in dose estimation. Considering the ^{131}I, the self-absorption S-values calculated by Geant4-DNA were almost 1.5 time larger than corresponding MIRD values. However, point by point comparison reveals that when the magnitudes of S-values are small, MIRD values are higher than Gean4-DNA corresponding values but with increasing the magnitudes S-values the Geant4-DNA become higher. For ^{177}Lu the situation is quantitatively the same. Regarding the cross-absorption, the relative deference (RD%) changes dramatically with source region (cell surface, cytoplasm and nucleus). Figure 4 clearly shows that with increasing the size of source region (cell/nucleus) and decreasing the magnitude of S-values, the relative difference increases for ^{131}I and ^{177}Lu. However, the relative difference for ^{90}Y data is almost constant and is independent of the region size. However the difference of slope between ^{90}Y and that observed by the ^{131}I and ^{177}Lu is due to the difference in energy and spectrum of radiations.

This is not the first time that such inconsistency is reported. Cai et al. used MCNP Monte Carlo code for calculation of cellular S-values for ^{111}In and reported 66-153% difference between their results and MIRD published values [21]. Bousis et al. also estimated cellular S-value of monoenergetic electron by their in-house Monte Carlo code and reported -80% to +86% systemic differences compared to the MIRD data [31]. Although MCNP may not be a proper Monte Carlo code for such simulations and in-house codes are not very well validated; however, the reported differences are too high to be blamed on such issues. We have to considered that, in Monte Carlo simulation codes the physical models and cross sections are constant and are not geometry dependent;while, in analytical calculations, geometry is essential and with a small change in geometry the calculation algorithms changes dramatically.

CONCLUSION

The results of present study showed a significant difference between the S-values from Geant4-DNA and corresponding MIRD data. The differences are most probably a reflection of systematic error and are not due to statistical fluctuation. Although we cannot definitely reprove the MIRD data however, Geant4-DNA is a very well validated Monte Carlo package and have been used for transport of electrons successfully.

REFERENCES

1. Chatal JF, Hoefnagel CA. Radionuclide therapy. Lancet. 1999 Sep 11;354(9182):931-5.
2. Dearling JL, Pedley RB. Technological advances in radioimmunotherapy. Clin Oncol (R Coll Radiol). 2007 Aug;19(6):457-69.
3. Buchsbaum DJ. Experimental radioimmunotherapy. Semin Radiat Oncol. 2000 Apr;10(2):156-67.
4. Bousis C, Emfietzoglou D, Nikjoo H. Monte Carlo single-cell dosimetry of I-131, I-125 and I-123 for targeted radioimmunotherapy of B-cell lymphoma. Int J Radiat Biol. 2012 Dec;88(12):908-15.

5. Bardiès M, Myers MJ. Computational methods in radionuclide dosimetry. Phys Med Biol. 1996 Oct;41(10):1941-55.

6. Goddu SM, Rao DV, Howell RW. Multicellular dosimetry for micrometastases: dependence of self-dose versus cross-dose to cell nuclei on type and energy of radiation and subcellular distribution of radionuclides. J Nucl Med. 1994 Mar;35(3):521-30.

7. Humm JL. Dosimetric aspects of radiolabeled antibodies for tumor therapy. J Nucl Med. 1986 Sep;27(9):1490-7.

8. Bardiès M, Chatal JF. Absorbed doses for internal radiotherapy from 22 beta-emitting radionuclides: beta dosimetry of small spheres. Phys Med Biol. 1994 Jun;39(6):961-81.

9. Humm JL. A microdosimetric model of astatine-211 labeled antibodies for radioimmunotherapy. Int J Radiat Oncol Biol Phys. 1987 Nov;13(11):1767-73.

10. Emfietzoglou D, Bousis C, Hindorf C, Fotopoulos A, Pathak A, Kostarelos K. A Monte Carlo study of energy deposition at the sub-cellular level for application to targeted radionuclide therapy with low-energy electron emitters. Nucl Instrum Meth B. 2007;256(1):547-53.

11. Budinger TF, Murty GS. MIRD cellular S values: Self-absorbed dose per unit cumulated activity for selected radionuclides and monoenergetic electron and alpha particle emitters incorporated into different cell compartments. Reston, Va: Society of Nuclear Medicine; 1997.

12. Sgouros G. Dosimetry of internal emitters. J Nucl Med. 2005 Jan;46 Suppl 1:18S-27S.

13. Loevinger R, Budinger TF, Watson EE. MIRD primer for absorbed dose calculations. New York: Society of Nuclear Medicine; 1988.

14. Cole A. Absorption of 20-eV to 50,000-eV electron beams in air and plastic. Radiat Res. 1969 Apr;38(1):7-33.

15. Eckerman KF, Westfall RJ, Ryman JC, Cristy M. Nuclear decay data files of the dosimetry research group. ORNL/TM-12350. Oak Ridge, TN: Oak Ridge National Laboratory; 1993.

16. Bousis C, Emfietzoglou D, Hadjidoukas P, Nikjoo H. A Monte Carlo study of absorbed dose distributions in both the vapor and liquid phases of water by intermediate energy electrons based on different condensed-history transport schemes. Phys Med Biol. 2008 Jul 21;53(14):3739-61.

17. Bernal MA, Liendo JA. An investigation on the capabilities of the PENELOPE MC code in nanodosimetry. Med Phys. 2009 Feb;36(2):620-5.

18. Champion C, Zanotti-Fregonara P, Hindié E. CELLDOSE: a Monte Carlo code to assess electron dose distribution--S values for 131I in spheres of various sizes. J Nucl Med. 2008 Jan;49(1):151-7.

19. Emfietzoglou D, Kostarelos K, Hadjidoukas P, Bousis C, Fotopoulos A, Pathak A, Nikjoo H. Subcellular S-factors for low-energy electrons: a comparison of Monte Carlo simulations and continuous-slowing-down calculations. Int J Radiat Biol. 2008 Dec;84(12):1034-44.

20. Syme AM, Kirkby C, Riauka TA, Fallone BG, McQuarrie SA. Monte Carlo investigation of single cell beta dosimetry for intraperitoneal radionuclide therapy. Phys Med Biol. 2004 May 21;49(10):1959-72.

21. Cai Z, Pignol JP, Chan C, Reilly RM. Cellular dosimetry of (111)In using monte carlo N-particle computer code: comparison with analytic methods and correlation with in vitro cytotoxicity. J Nucl Med. 2010 Mar;51(3):462-70.

22. Nikjoo H, Uehara S, Emfietzoglou D, Cucinotta FA. Track-structure codes in radiation research. Radiat Meas. 2006;41(9-10):1052-74.

23. Incerti S, Baldacchino G, Bernal M, Capra R, Champion C, Francis Z, Guatelli S, Gueye P, Mantero A, Mascialino B, Moretto P, Nieminen P, Rosenfeld A, Villagrasa C, Zacharatou C. The Geant4-DNA project. Int J Model Simul Sci Comput. 2010;1(02):157-78.

24. Eckerman KF, Endo A. MIRD: Radionuclide Data and Decay Schemes. Reston, Va: Society of Nuclear Medicine; 1989.

25. Agostinelli S, Allison J, Amako Ka, Apostolakis J, Araujo H, Arce P, Asaig M, Axen D, Banerjee S, Barrand G, Behner F, Bellagamba L, Boudreau J, Broglia L, Brunengo A, Burkhardt H, Chauvie S, Chuma J, Chytracek R, Cooperman G, Cosmo G, Degtyarenko P, Dell'Acqua A, Depaola G, Dietrich D, Enami R, Feliciello A, Ferguson C, Fesefeldt H, Folger G, et al. GEANT4—a simulation toolkit. Nucl Instrum Meth A. 2003;506(3):250-303.

26. Incerti S, Ivanchenko A, Karamitros M, Mantero A, Moretto P, Tran HN, Mascialino B, Champion C, Ivanchenko VN, Bernal MA, Francis Z, Villagrasa C, Baldacchin G, Guèye P, Capra R, Nieminen P, Zacharatou C. Comparison of GEANT4 very low energy cross section models with experimental data in water. Med Phys. 2010 Sep;37(9):4692-708.

27. Francis Z, Incerti S, Karamitros M, Tran HN, Villagrasa C. Stopping power and ranges of electrons, protons and alpha particles in liquid water using the Geant4-DNA package. Nucl Instrum Meth B. 2011;269(20):2307-11.

28. Incerti S, Psaltaki M, Gillet P, Barberet P, Bardiès M, Bernal MA, Bordage MC, Breton V, Davidkova M, Delage E, El Bitar Z, Francis Z, Guatell S, Ivanchenko A, Ivanchenko V, Karamitros M, Lee SB, Maigne L, Meylan S, Murakami K, Nieminen P, Payno H, Perrot Y, Petrovic I, Pham QT, Ristic-Fira A, Santin G, Sasaki T, Seznec H, Shin JI, et al. Simulating radial dose of ion tracks in liquid water simulated with Geant4-DNA: A comparative study. Nucl Instrum Meth B. 2014;333:92-8.

29. André T, Morini F, Karamitros M, Delorme R, Le Loirec C, Campos L, Champion C, Groetz JE, Fromm M, Bordage MC, Perrot Y, Barberet Ph, Bernal MA, Brown JMC, Deleuze MS, Francis Z, Ivanchenko V, Mascialino B, Zacharatou C, Bardiès M, Incerti S. Comparison of Geant4-DNA simulation of S-values with other Monte Carlo codes. Nucl Instrum Meth B. 2014;319:87-94.

30. Champion C, Incerti S, Perrot Y, Delorme R, Bordage MC, Bardiès M, Mascialino B, Tran HN, Ivanchenko V, Bernal M, Francis Z, Groetz JE, Fromm M, Campos L. Dose point kernels in liquid water: an intra-comparison between GEANT4-DNA and a variety of Monte Carlo codes. Appl Radiat Isot. 2014 Jan;83 Pt B:137-41.

31. Bousis C, Emfietzoglou D, Hadjidoukas P, Nikjoo H. A Monte Carlo study of cellular S-factors for 1 keV to 1 MeV electrons. Phys Med Biol. 2009 Aug 21;54(16):5023-38.